Shahrood University of Technology

Journal of Mining and Environment (JME)

Journal homepage: www.jme.shahroodut.ac.ir

Iranian Society of Mining Engineering (IRSME)

Landslide Susceptibility Mapping: Comparison of Knowledge-driven AHP-FR and Data-driven SVM Methods in Zarab-Sanandaj Sub-basins, Kurdistan, Iran

Sarina Akbari[1], Reza Ghezelbash[2*], Hamidreza Ramazi[1], and Abbas Maghsoudi[1]

1. Faculty of Mining Engineering, Amirkabir University of Technology, Tehran, Iran
2. College of Engineering, University of Tehran, Tehran, Iran

Article Info

Received 25 September 2024
Received in Revised form 11 April 2025
Accepted 5 May 2025
Published online 5 May 2025

DOI: 10.22044/jme.2025.15122.2890

Keywords

Landslide, Analytical hierarchy process
Frequency ratio
Support vector machine
Kurdistan

Abstract

Natural hazards, particularly landslides, have long posed significant threats to people, buildings, and the surrounding environment. Therefore, comprehensive planning for urban and rural development necessitates the development and implementation of landslide risk zoning models. Numerous methodologies have been proposed for generating landslide hazard maps, which can potentially aid in predicting future landslide-prone areas. This study employed an integrated approach that combines statistical and multi-criteria decision-making (MCDM) methodologies. The Frequency Ratio (FR) and Analytical Hierarchy Process (AHP) were utilized as knowledge-driven approaches, while the Support Vector Machine (SVM) using an RBF kernel, a widely recognized machine learning algorithm, was applied as a data-driven method. Ten factors influencing landslides were considered, including slope angle, aspect, altitude, geology, land use, climate, erosion, and distances from rivers, faults, and roads. The results revealed that landslides are more predictable in the southern, southwestern, and central regions of the studied area. A quantitative assessment of the different methods using prediction-rate curves indicated that the SVM method outperformed the FR and AHP-FR approaches in identifying susceptible areas. The findings of this work could be effectively employed to mitigate potential future hazards and associated damages.

1. Introduction

Natural hazards have always posed a significant threat to both people and property, often resulting in substantial damage to buildings and the environment. Among environmental risks such as storms, floods, avalanches, erosion, and tsunamis, earthquakes and landslides constitute one of the most destructive categories of natural hazards worldwide [126]. Characterized by steep slopes and loose soil, hilly and mountainous regions are particularly vulnerable to landslides, with the majority of such events occurring within these specific terrains. It is estimated that landslides cause approximately 600 deaths annually [92]. Studies indicate that at least 17% of fatalities resulting from natural disasters are directly attributable to landslide occurrences [92]. To address these hazards and reduce their impact on both the economy and human lives, it is imperative to enhance landslide preparedness through the prediction of potential occurrences and the identification of high-risk areas. Landslide inventory and susceptibility modeling serve as critical preliminary steps in efforts aimed at forecasting and mitigating the risks associated with such phenomena [41], [42].

A landslide vulnerability map serves as a critical tool for understanding and predicting future landslides, as well as minimizing their associated impacts. Over the past three decades, advancements in Geographic Information Systems (GIS) and remote sensing technologies, along with the development and implementation of various

Corresponding author: r.ghezelbash@ut.ac.ir (R. Ghezelbash)

strategies to assess landslide hazard, risk, and susceptibility, have made such analyses increasingly practical and effective [4], [16], [39], [60], [75], [99], [100], [109], [114]. For instance, Bhardwaj and Singh in (2023) conducted a comprehensive review on landslide susceptibility assessment using these methods, highlighting their growing significance in geospatial analysis. Similarly, Dhakal and Singh in (2025) employed a geospatial approach to assess landslide susceptibility in the Spiti region of India, demonstrating the applicability of advanced mapping techniques in diverse geographical settings.

Despite the wide array of techniques that have been proposed and investigated, there is currently no universally accepted or standardized methodology for establishing landslide vulnerability models [41], [42]. In general, the methods applied in this field can be classified into qualitative and quantitative categories. Qualitative methods are characterized by their subjective nature and exploratory approach to evaluating landslide susceptibility [2]. In contrast, quantitative approaches encompassing both deterministic and statistical techniques rely on numerical expressions to determine the relationships between controlling parameters and landslide occurrences [45], [101], [119]. A variety of quantitative techniques have been frequently utilized, including logistic regression [53], [98], Bimodal statistical investigation [3], [27], multivariate logistic regression [80], multivariable adaptable regression splines [43], [90], discriminant analysis [38], weight of evidence [23], [55], and evidential belief functions [59], [89]. In addition, knowledge-driven Multi-Criteria Decision-Making (MCDM) methods such as TOPSIS, VIKOR [7], and Analytic Hierarchy Process (AHP) have also been widely applied [5], [6], [34], [64], [68], [122].

Given the growing complexity and diversity of geospatial data, the comparison of these methodologies becomes crucial for determining the most effective approach in predicting and mitigating landslide risks.

To enhance the robustness of modeling frameworks, hybrid strategies that combine knowledge-based and data-driven techniques have gained popularity. Among the latter, the Frequency Ratio (FR) method has been used extensively due to its simplicity and strong performance in estimating the influence of causative factors on landslide occurrences [1], [54], [67], [76].

More recently, Artificial Intelligence (AI)-based approaches have become increasingly prominent in landslide susceptibility modeling. Among these, Machine Learning (ML) methods such as Artificial Neural Networks (ANN), Support Vector Machines (SVM), and Random Forest (RF) have been recognized for their ability to capture complex nonlinear relationships within high-dimensional datasets.

Many researchers have utilized these methods over the years for predicting landslide occurrences as well as other studies related to Earth sciences. For example, Alimoradi et al. in (2011) utilized this method, demonstrating that Artificial Neural Networks (ANN) can significantly enhance the accuracy of shear wave velocity predictions, which can be considered an effective tool for geotechnical and engineering applications. In another study conducted by Alimoradi et al. in (2011), the researchers also utilized Artificial Neural Networks (ANN) to solve magnetic inversion problems. By training a three-layer feedforward neural network with synthetic data, they were able to predict the depth of dikes with acceptable accuracy. This method was applied to magnetic field data from the Kermian region in Iran, and the results were compared with real borehole data, demonstrating the network's effectiveness in estimating dike depth. Additionally, in a more recent study by Ghasemi Tabar et al. (2023), the researchers employed machine learning techniques and Python programming for intelligent borehole simulation. They utilized algorithms such as Artificial Neural Networks to process and simulate borehole data, improving decision-making processes in mining operations by providing accurate predictions of subsurface geological features.

Furthermore, a comparative study by Mohammadi and Hezarkhani (2020) explored the effectiveness of Support Vector Machine (SVM) and Random Forest (RF) methods in classifying alteration zones using remotely sensed data. Their findings demonstrated that SVM outperformed RF, offering higher accuracy in identifying alteration zones, a result that underscores the growing potential of machine learning methods in geoscientific applications. Similarly, Alimoradi et al. in (2013) applied both Artificial Neural Networks (ANN) and Support Vector Machines (SVM) to estimate carbonate pore sizes from 3D seismic data. Their study demonstrated how these machine learning techniques can be effectively used for accurate subsurface property estimation, further highlighting their versatility in addressing complex geological and geophysical challenges.

Kavzoglu et al. (2014) compared the performance of SVM with other classifiers for landslide susceptibility mapping and found that SVM yielded higher accuracy and more reliable results. Similarly, Lee et al. (2017) applied SVM to landslide susceptibility modeling and concluded that the algorithm outperformed ANN and other traditional methods, demonstrating its robustness in capturing complex, non-linear relationships in geospatial data. In recent years, SVM has also proven effective in predicting areas favorable to mineralization, as demonstrated by Akbari et al. (2025), who combined SVM with optimization algorithms for better prediction of porphyry-copper mineralization zones. These findings suggest that SVM consistently provides high accuracy in various geospatial and geotechnical tasks. These findings suggest that the SVM algorithm, when implemented with a Radial Basis Function (RBF) kernel, has notably demonstrated excellent performance in spatial prediction tasks by effectively transforming the input space and identifying optimal decision boundaries. So, it is often the method of choice when dealing with challenging geospatial and environmental datasets, reaffirming its utility and effectiveness in a wide range of applications.

Kurdistan is a mountainous province that contains many both stable and unstable slopes. The phenomenon of significant and widespread downslope movement of materials causes landslides in certain parts of the province, leading to devastating impacts on agricultural lands, road networks, and residential areas notably along the Sanandaj–Marivan and Sarvabad–Kamyaran transportation axes.

Accordingly, the primary objective of this work is to assess the relationship between landslide occurrences and their contributing factors using a combination of traditional and advanced modeling techniques. Initially, knowledge-driven methods such as the Analytical Hierarchy Process (AHP), and data-driven statistical approaches like the Frequency Ratio (FR) were applied to generate preliminary susceptibility maps. To improve the predictive accuracy and capture the inherent complexity and non-linear interactions among the causative variables, the Support Vector Machine (SVM) algorithm [61], [62], [74], [35], [82], [86], [87], was employed as an artificial intelligence-based model. In this regard, a Radial Basis Function (RBF) kernel was utilized, which enables the SVM to effectively map input data into a higher-dimensional feature space, enhancing its capability to distinguish between landslide-prone and stable areas. Finally, the performance of all three approaches was evaluated and compared using quantitative metrics to identify the most accurate and efficient model for landslide susceptibility mapping. This hybrid framework highlights the growing potential of machine learning in geoscientific analyses and offers a valuable tool for risk assessment and spatial planning in landslide-prone regions.

2. Studied Area

The studied area is situated in the southwestern region of Kurdistan Province and includes the Zarab and Sanandaj sub-basins, located in the western part of Iran (Figure 1a). The selected area covers approximately 7,445 km², extending 133 kilometers in the east–west, and 106 kilometers in the north–south direction. This region is characterized by mountainous and rugged terrain (Figure 1b).

Abundant precipitation contributes to intensive erosion, primarily through surface runoff, which has resulted in the formation of dome-shaped landforms with gentle slopes and broad valleys. Consequently, a significant portion of the area is marked by eroded dome-like mountains, as well as parallel and consecutive mountain ranges with steep inclines. The lithology of the region is predominantly sedimentary, particularly limestones. The formation of these rugged features is attributed to late Tertiary orogenic activities, followed by extensive erosion during the Quaternary period, which has shaped the area into its current geomorphological form. From a geological perspective, the majority of the area consists of Cretaceous rock units, while Eocene and Oligo-Miocene formations are widespread in the central parts. In contrast, Quaternary deposits are sparsely distributed near the marginal zones of the region (Figure 1a). Approximately 100,492 hectares of the studied area are utilized for agricultural purposes. According to the Iran Meteorological Organization, Kurdistan has a Mediterranean climate, with cold winters and warm summers in the central and eastern areas, and a moderate climate in the western region. The mean annual temperature is around 13.4°C.

3. Spatial Dataset and Landslide Conditioning Criteria

3.1. Slope angle factor

The slope angle is regarded as a key parameter in the analysis of slope stability [92]. Its inclusion in landslide hazard modeling is a widely adopted

practice due to its strong association with landslide occurrences. Previous studies have shown that landslides predominantly occur on peaks, hills, steep slopes, and ridges, whereas plains exhibit the lowest frequency of landslide events [39], [102].

In this study, the slope angle map of the investigation area was generated using a Digital Elevation Model (DEM) and subsequently classified into four distinct slope categories (Figure 2a).

3.2. Aspect factor

Aspect has been recognized as a critical geomorphological parameter influencing the occurrence of landslides, as thoroughly documented in numerous studies [78], [92], [110], [129]. The likelihood of landslides may be influenced by various climatic factors, such as solar radiation, precipitation intensity, and the orientation and morphology of slopes. In particular, the degree of hillslope saturation resulting from heavy rainfall is significantly governed by the infiltration capacity of the slope, which depends on multiple variables including topography, soil type, permeability, porosity, moisture content, organic matter, land cover, and the prevailing climatic conditions. These factors collectively contribute to variations in the capillary water pressure within slope materials.

In the current study, a detailed aspect classification map of the region was developed to explore the spatial relationship between slope orientation and landslide distribution (Figure 2b). The slope aspects were categorized into nine classes, namely: flat, north (N), south (S), west (W), east (E), southeast (SE), southwest (SW), northeast (NE), and northwest (NW).

3.3. Altitude factor

Another relevant controlling factor considered in this work is altitude. The higher the altitude, the more susceptible the area becomes to landslides, because at high altitudes, rocks are more weathered and the melting and freezing phenomena are predominant [32], [85]. Since altitude has a vital effect on the incidence of landslides, it has been applied by researchers to generate landslide sensitivity models around the globe [58], [96]. In line with this, the altitude map of the studied area was prepared to analyze its relationship with landslide occurrences (Figure 2c).

3.4. Lithological factor

The lithological condition of the land plays a significant role in the landslide phenomenon, which is studied as part of geomorphology. There is a significant need for data from lithological units in susceptibility studies due to the fact that they have widely varying landslide susceptibility values. In this regard, the proper division of the lithological characteristics is necessary [63], [128]. The geological map of the research district, developed by the Geological Survey of Iran (GSI), was utilized and digitized within a Geographic Information System (GIS) to extract lithological data for the analysis (Figure 2d).

3.5. Land use factor

This research work employed a guided categorization technique to delineate and categorize six distinct land use patterns. These grouped land uses are as follows: Agriculture, Forest, Island, Rangeland, Urban, and Waterland areas (Figure 2e). A predominant feature of the studied district is the prevalence of farmlands. It is generally accepted that land use and the extent of vegetation coverage play a crucial role in the stability of slopes [83]. The conversion of forested areas to agricultural lands, followed by landslide events, represents a critical sequence highlighting the significance of land use in the incidence of landslides. Tree cover can remove water from the soil through high evapotranspiration, thereby reducing the influence of soil moisture levels, as the presence of water within the soil mass is one of the effective parameters in reaching saturation and triggering landslides. In addition, tree cover, with its deep and continuous root systems, can enhance the mechanical stability of the soil mass on slopes.

3.6. Climate factor

The parameters including geology, slope, altitude, precipitation, and human activities are commonly considered in landslide studies. While these factors play a major role in the occurrence of this phenomenon, various studies have shown that the distribution of landslides is also influenced by climate change, which has a significant impact on triggering land instability. According to previous research, most landslides occur in cold and humid climates, whereas a small percentage are reported in arid environments. Based on one of the geomorphic-zoning methods, the research area is classified into four distinct climatic zones, each with specific geomorphic characteristics that exert both direct and indirect effects on landslide occurrence (Figure 2f).

3.7. Erosion factor

The erosion rate of the research region is another influential factor contributing to the incidence of landslides. According to previous studies, erosion is one of the variables that exert the most substantial impact on landslide occurrences. The higher the erosion intensity in an area, the more prone the land is to landslide events. The rate of erosion, therefore, is directly associated with the probability of landslides. To determine the effect of erosion in the studied area, its map was prepared and categorized into seven sections, showing the intensity of erosion from very low to very high (Figure 2g).

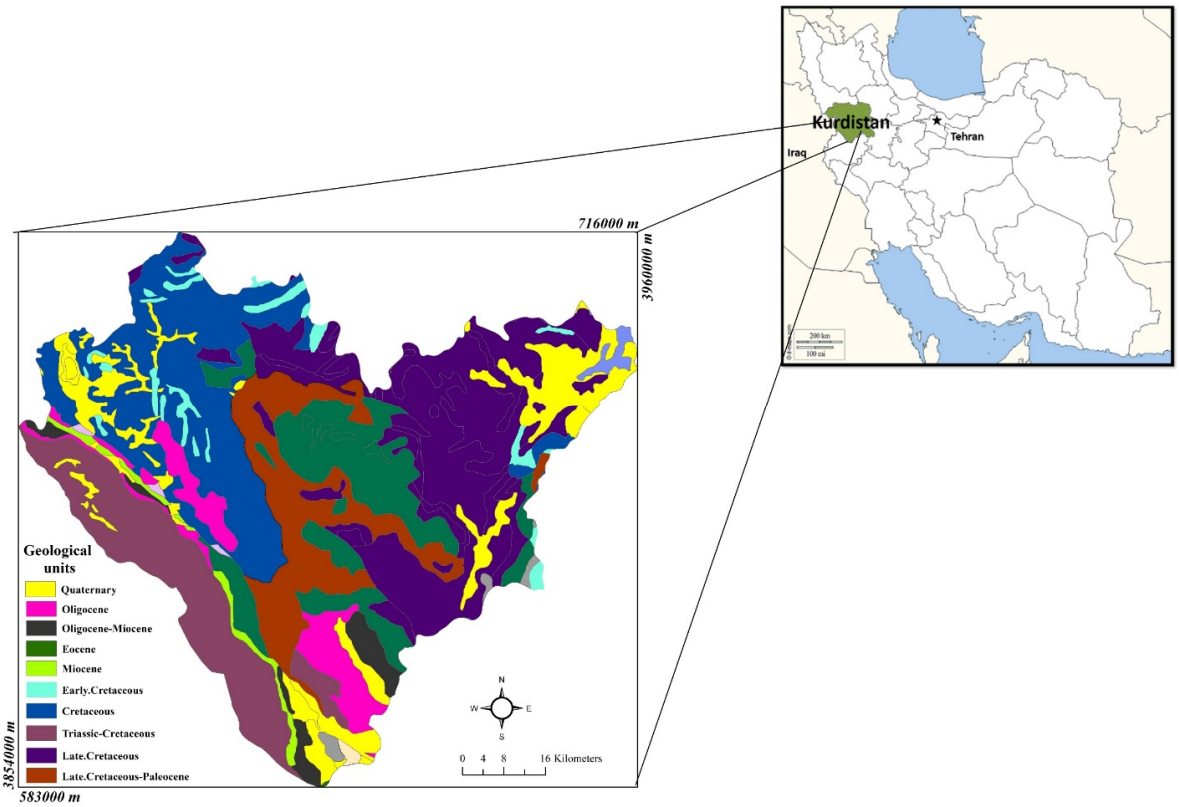

(a)

(b)

Figure 1. (a) The location and the geological map of the studied area in the Kurdistan province, Iran; (b) landscape picture of the area of study.

3.8. Distance to rivers factor

An essential factor in determining how consistently a slope behaves is the rate of saturation of the material comprising the incline [122], [123]. Another important factor is the slope's closeness to infrastructure for drainage in terms of sustainability. The erosion of slopes and the saturation of the lower portion of the material, along with the increasing water levels due to streams, may adversely affect the stability [52], [53]. To assess the impact of streams on slopes, five different buffer zones of rivers, with 500 m intervals, were generated within the studied area (Figure 2h). A Euclidean distance technique was implemented to conduct a visual detection to establish the correlation between the presence of a river and the frequency of landslides.

3.9. Distance to the faults factor

Fault is one of the most significant tectonic parameters that causes slope sensitivity by causing fractures and detachments in the rocks, making them easier to move. The higher the density of these fractures, the higher the sensitivity of the rock to various forms of erosion, especially landslides [36]. Generally, the greater the distance from the fault, the lower the likelihood of a landslide occurring. Along fault planes, the mechanisms of erosion and water flow contribute to the facilitation of landslides. Accordingly, in most slope instability studies, the fault factor is widely recognized as a substantial component affecting the occurrence rate of landslides. In this context, a visual detection was conducted to determine the connection between faults and landslides through the application of the Euclidean distance approach. The map depicting the distances to faults was created by employing the reported faults on the geological map (Figure 2i) at intervals of 1000 meters.

3.10. Distance to roads factor

Distance to the existing roads can also affect landslides, just like the distance to rivers. Roads have the ability to function as a barrier for water flow, a net source, or an aisle for the movement of water. Also, they are generally considered the origin of landslides, depending on their location in the mountains [57]. The development of roads and side soil erosion are significant causes of slope instability and landslides. In general, roads disturb the natural position of the slope and cause vertical cuts in the terrain, which increases the pressure on the lower part of the road. Additionally, human activities for road construction, such as excavation and embankment, lead to changes in drainage and hydrology, ultimately impacting stress and slope balance. Due to this rationale, the incorporation of roadways is deemed necessary in landslide susceptibility modeling. In this regard, to determine the impact of the distance from roads on the stability of the slope and landslide susceptibility, five distinct sectors are created along the trajectory of the road (Figure 2j).

4. Material and Methods

4.1. Analytical Hierarchy Process (AHP)

For solving multimodal decision-making issues, AHP [103] is a widely used MCDM approach that has been suggested and further developed [5], [9]. Put simply, this methodology significantly contributes to the resolution of intricate decision-making challenges by decomposing the problem into a network of hierarchies comprising linked decision components. This is achieved through a pairwise evaluation of the significance of various criteria and respective sub-criteria. The AHP procedure for multi-criteria decision-making involves the following three primary steps:

1) Creating a hierarchical structure.

2) Pair-wise comparison of criteria and alternatives.

3) Rating-based integration.

The first and last levels of the hierarchical structure are related to the purpose of the study and the alternative structure, respectively, while the middle level is related to the criteria and sub-criteria. In this method, the elements of the middle level are paired according to the table proposed by Saaty in (1994). Using this table, qualitative judgments can be converted into numerical values and rank the criteria and sub-criteria based on pairwise comparisons of important dependencies with respect to the purpose of the decision.

In the current research, AHP has been employed to identify the significance of effective parameters in landslide susceptibility mapping. The determination of interrelated variable values is often contingent upon the discretion of the decision maker.

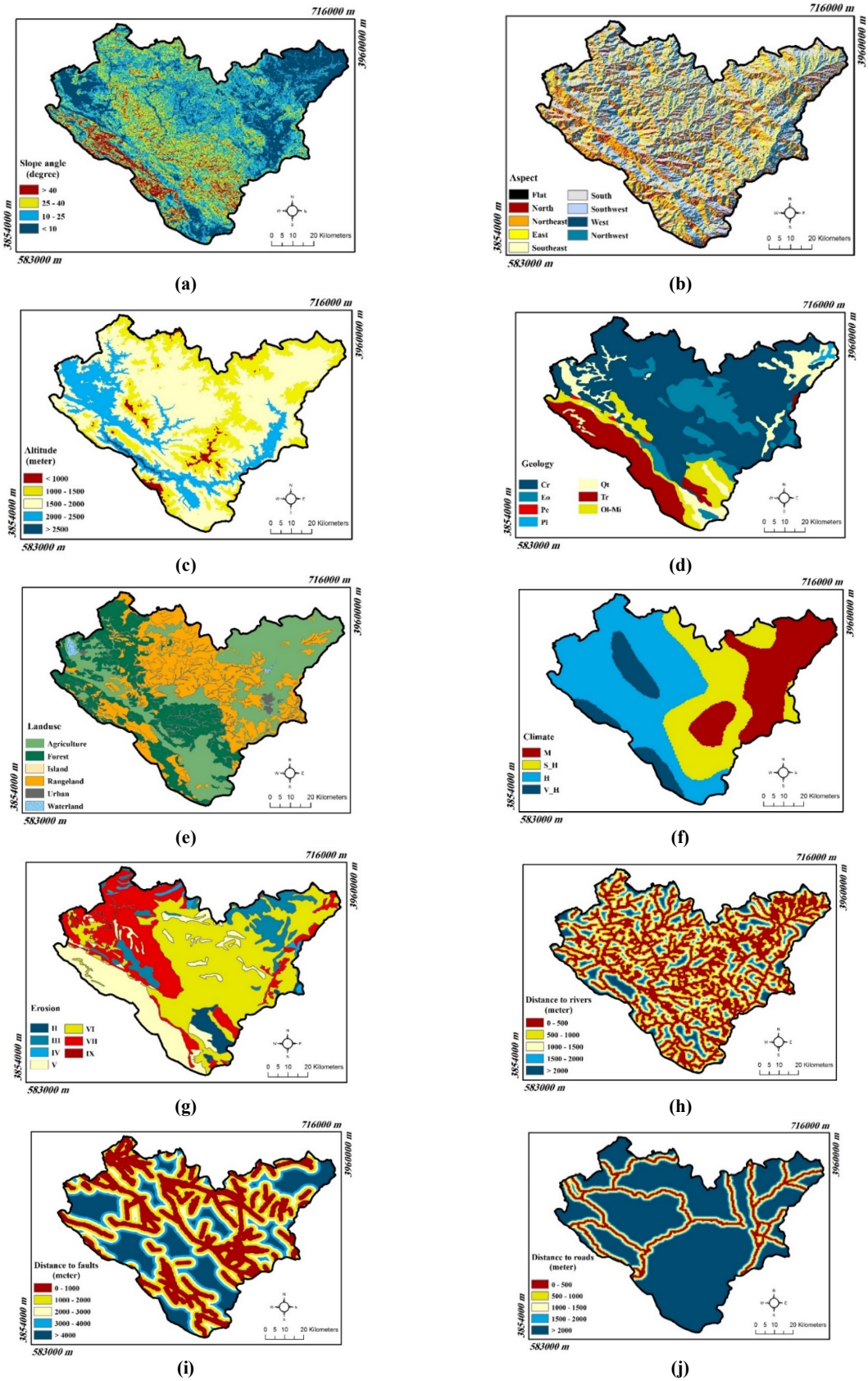

Figure 2. Landslide condition factors: (a) Slope, (b) Aspect, (c) Altitude, (d) Lithology, (e) Land use, (f) Climate, (g) Erosion, (h) Distance to rivers, (i): Distance to faults and (j) Distance to road.

4.2. Frequency Ratio (FR)

Because of determining the frequency ratio of each element that influences the occurrence of landslides, the utilization of a Geographic Information System (GIS) has been employed. This involves the integration of the models representing each variable with the map representing the landslide indices. By doing so, the proportion of pixels within the research region that exhibit landslides and those that do not may be computed. Following the equation FR = A/B, the frequency ratio of landslide to non-landslide spots was obtained for variable classes. In the present context, FR shows the frequency ratio, and the classification of pixels as landslides is denoted by the variable A, whereas the fraction of pixels categorized as non-landslides is represented by the variable B. In the context of connection analysis, the ratio pertains to the proportion of the region affected by landslides in relation to the whole district under consideration.

Consequently, a value in close proximity to 1 signifies an average value. In contrast, numbers over 1 indicate a stronger association, while values below 1 indicate a weaker correlation.

The FR technique is employed to elucidate the relation among the distribution of landslides and the parameters affecting them [93], [94], [97].

4.3. Support Vector Machine (SVM)

The SVM algorithm, using the RBF kernel has utilized to assess the likelihood of landslides within the research region. The results obtained from this analysis were subsequently compared. The SVM has been utilized for both classification and regression tasks. The classification methodology utilized in this method is derived from the concept of statistical learning [31], [117]. Based on the theoretical framework proposed, the error rate of a learning machine when applied to unclassified data could be regarded as the generalized rate of error. The coefficients presented herein are dependent on the total training error rates, serving as indicators of the level of sophistication exhibited by the classification algorithms. In order to minimize the occurrence of generalized errors, it is important to decrease both the degree of training error and the level of sophistication of the classifier. One approach to achieve this objective is to optimize the separation margin.

In turn, this machine learning approach proves to be advantageous since the segregation buffer is unaffected by the dimensions of the incoming data. The SVM algorithm, which has gained significant popularity over the past twenty years, relies on nonlinear synchronous transmission with a considerable specific spatial dimension [117]. The two-class SVM model is described in the following manner [124]:

Considering a collection of separate linear training cells:

$$X_i (i = 1,2,...,n) \quad (1)$$

The training cells including two distinct divisions specified as $y_i = \pm 1$. The aim of SVM modelling is identifying an N-dimensional segregation outline in two divisions that characterized by their maximum slit. This can be mathematically be described as:

$$\tfrac{1}{2}\|W\|^2 \quad (2)$$

According to aforementioned limitations:

$$Y_i((w x_i)+b) \geq 1 \quad (3)$$

where $\|W\|$ is the standard hyperplane, and b is a scalar base using Lagrange multivariate, the performance computation value can define:

$$L = \frac{1}{2}\|w\|^2 - \sum_{i=1}^{n} \lambda_i (y_i((w x_i)+b)-1) \quad (4)$$

Where λ_i is a Lagrange multiplier. Optimum weights of hyperplane, denoted as w, can be represented as a linear arrangement of the training points $\tfrac{1}{2}\|W\|^2$ and $X_i (i = 1,2,...,n)$:

$$y_i((w x_i)+b) \geq 1-\varepsilon_i \quad (5)$$

Eq. (4) now becomes:

$$L = \frac{1}{2}\|w\|^2 - \frac{1}{vn}\sum_{i=1}^{n} \varepsilon_i \quad (6)$$

Polynomial kernels as well as the RBF [96], [121], often known as the Gaussian kernel, are the most common types of kernels applied for SVM classification tasks.

To deal with the non-linearity of the issue, this research employs a Gaussian kernel (Eq. (4)) due to its good generalizing capabilities. Furthermore, RBF provides superior predictive capabilities for landslide prospectivity modeling than alternative kernels in many studies and situations (particularly in nonlinear problems) [96], [121], [111].

$$k(x,y) = \exp(-\gamma \|x-y\|^2) \quad (7)$$

5. Results and Discussion

5.1. Collection and preparation of various evidence layers

As mentioned before, to develop a landslide zoning model, it is essential to take into account parameters influencing the incidence of landslides. Determining these features is usually established by domain professionals. These characteristics are Slope angle, Aspect, Altitude, Geology, Land use, Climate, Erosion, Distance to rivers, faults, and roads. To carry out the research work, descriptive layers of every factor were prepared in the studied region. In order to achieve this objective, the DEM map and the roads in the region were obtained from the 1:25,000 topographic map of the research area, using ArcGIS software. The faults, which have a significant effect on landslide prediction, were also derived from the 1:100,000 geological map of the studied area. The lithological data utilized in the present research were acquired from preexisting geological maps of the region, which were available at a scale of 1:250,000 and categorized based on distinct geological units. In this regard, all lithological groups were classified into 7 groups. Moreover, climate conditions were classified into 4 groups, which have different effects on landslides.

Several processes were carried out on different layers that indicate different effective factors in landslide susceptibility, using ArcGIS software (Figure 2). Altitude is a significant element in regulating the extent and nature of erosion and human activities, hence influencing the susceptibility of an area to landslides (see Figure 2c). Additionally, slope and aspect maps have been extracted from DEM using Slope and Aspect tools, respectively, in ArcGIS software (Figure 2a, b). Lithological, land use, and climatic layers were transformed into raster values (Figure 2d, e, f). The distance from faults, rivers, and roads maps were generated using Euclidean distance (Figure 2h, i, j).

5.2. Landslide susceptibility mapping utilizing AHP-FR procedure

5.2.1. Calculation of criteria weights by AHP

Not all of the criteria used for landslide occurrence have the same effect. For this reason, each criterion can be assigned a weight. Many geoscience studies have used the AHP procedure to calculate the weight of the criteria. In the present investigation, the AHP model has been applied to assign an appropriate weight to each criterion. Existing sources and expert opinions were used to assign weights to the criteria. Higher weights are attributed to layers that have a greater role in landslide incidence. The weight of the layers varies from 1 to 9. The least effective component is given a value of 1, while the value of 9 is allocated to the most efficient one (Table 1). At this stage, to perform the comparison using the pair-wise comparison method, a decision matrix with dimensions of 10 × 10 was created, and different criteria, which are effective factors in landslides regardless of the sub-criteria and classes related to variables, were compared in pairs (Table 2). The geometric mean of the columns was divided to calculate the weight of each criterion. As shown in Table 2, four factors, distance from the river and fault, geology, slope, and land use, with weights of 0.23, 0.13, 0.13, 0.13, and 0.11, respectively, are considered the most important influential criteria in the risk of landslides in the region.

5.2.2. Calculation of sub-criteria weights by FR

This methodology operates under the supposition that forthcoming landslides manifesting under similar current conditions will resemble those observed in previous instances of landslides. The frequency ratio technique elucidates the relation among the spatial distribution pattern of landslides and the respective categories of parameters that contribute to their occurrence in the given area. The FR model employs a calculation to identify the weights of classes associated with each factor. This calculation is demonstrated by the equation FR = A / B, where FR represents the frequency ratio. A is the percentage of landslide spots, while B represents the percentage of non-landslide spots.

This study involved the calculation of FR values for specific divisions of 10 effective criteria. The quantity of landslides within each division was taken into account, ignoring the influence of the primary criteria. The results are found in Table 3. Subsequently, a landslide propensity map was generated utilizing the FR model (Figure 3).

Table 1. Scale proportions in the Analytical Hierarchy Process.

Significance score	Definition
1	Equal significance or privilege
2	Equal to moderate significance or privilege
3	Moderate significance or privilege
4	Moderate to intense significance or privilege
5	Intense significance or privilege
6	Intense to very intense significance or privilege
7	Very intense significance or privilege
8	Very to extremely intense significance or privilege
9	Extreme significance or privilege

Table 2. AHP technique pairwise comparison of ten criteria and their determined weights (Akbari et al., 2023).

Criteria	Geology	Land use	Climate	Erosion	Fault	River	Aspect	Altitude	Slope	Road	Weights
Geology	1.00	3	6	2	1	0.5	3	2	1	3	**0.13**
Land use	0.33	1	3	0.5	0.33	6	1	0.5	0.33	1	**0.11**
Climate	0.17	0.33	1	0.33	0.17	0.11	0.33	0.25	0.17	0.33	**0.02**
Erosion	0.5	3	3	1	0.5	0.25	2	1	0.5	2	**0.08**
Fault	1	3	6	2	1	0.5	3	2	1	3	**0.13**
River	2	0.17	9	4	2	1	6	4	2	6	**0.23**
Aspect	0.33	1	3	0.5	0.33	0.17	1	0.5	0.33	1	**0.04**
Altitude	0.5	2	4	1	0.5	0.25	2	1	0.5	2	**0.08**
Slope	1	3	6	2	1	0.5	3	2	1	3	**0.13**
Road	0.33	1	3	0.5	0.33	0.17	1	0.5	0.33	1	**0.04**

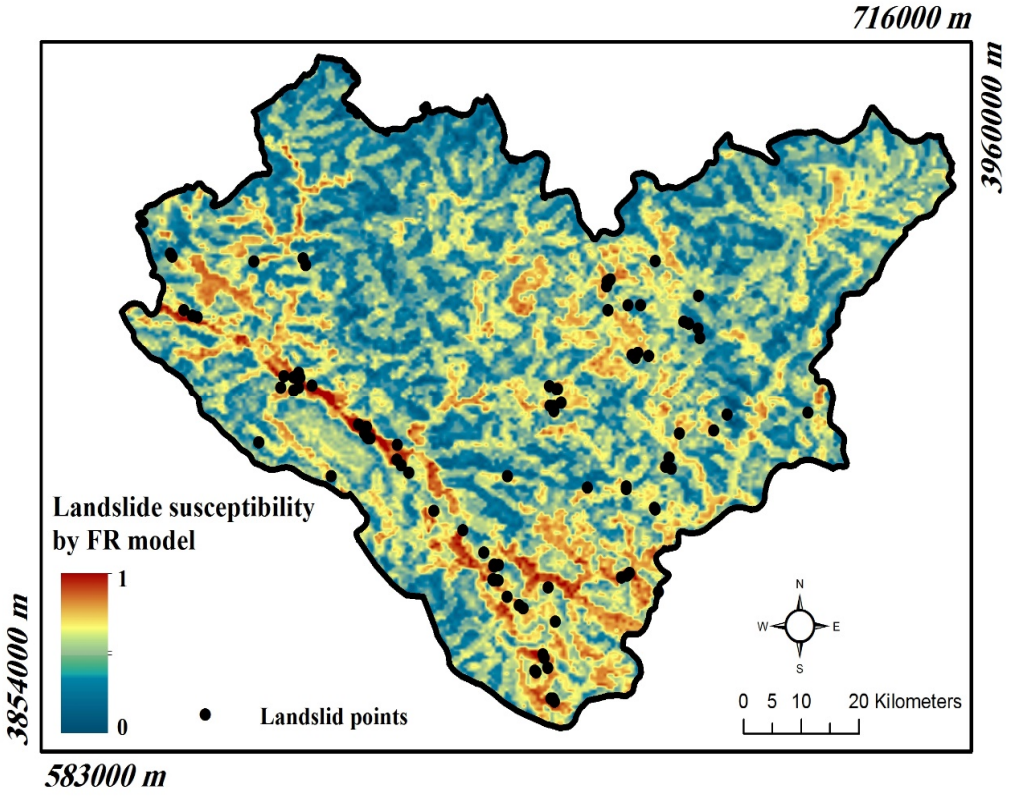

Figure 3. Landslide susceptibility map based on FR model.

To enhance the comprehension of the findings, values of FR were adjusted and transferred into the range of [0-1] (Table 3). In the analysis of the outcomes, the FR values close to 0 indicate lower correlation, while values closer to 1 indicate higher correlation.

According to Table 3, the outcomes indicate that the highest weights calculated for the classes

of geological factor belong to the geological units of Oligo-Miocene and Eocene ages, with FR values of 2.57 and 1.89, respectively. These classes cover 21.28% and 27.66% of the landslide locations within 8.26% and 14.63% of the areas, respectively. The study of the land use factor shows that the highest FR value is computed for agricultural land classes (FR=1.42) which predicted 53.19% of landslides within 37.38% of the area. The study of the climatic factor shows that the highest FR values belong to the areas with s semi-humid and humid climate with the values of 1.82 and 1.06, which cover 46.81% and 44.68% of landslides within 25.73% and 42.02% of the areas, respectively. For erosion factor, the highest FR value is 2 which covers 1.06% of the landslides within 0.53% of the total area and is related to class 9, while the next highest values are related to classes 5 and 6, forecasting 27.66% and 55.32% of landslides within 16.2% and 41.18% of the areas, respectively. The examination of linear elements, such as proximity to faults, rivers, and roadways, revealed that the initial categories of these variables exhibit the greatest FR ratios. Specifically, the obtained FR scores for the initial categories are 1.27, 1.25, and 1.91, respectively. Based on the findings pertaining to the Aspect and Slope elements, it can be shown that the highest FR scores are attained by classes linked to northward orientations and areas characterized by a slope angle below 10 degrees (specifically, 1.85 and 1.47, respectively). According to the results of the Altitude factor, elevations between 1000-1500m have the highest FR value (FR=2.58) covering 42.55% of landslides within 16.52 % of the entire area. More detailed information on other classes related to 10 factors influencing the occurrence of landslides can be found in Table 3.

5.2.3. Generation of predictive AHP-FR model

In the end, a model of landslide susceptibility was produced by employing the AHP weights for 10 key criteria (as shown in Table 2) and the FR values for their corresponding classes (as presented in Table 3) with the help of ArcGIS 10 software. The outcome of the landslide susceptibility map reveals the potential for landslides, presented as a continuum ranging from 0 to 1. The higher the value approaches 1, the more pronounced the vulnerability to landslides (Figure 4).

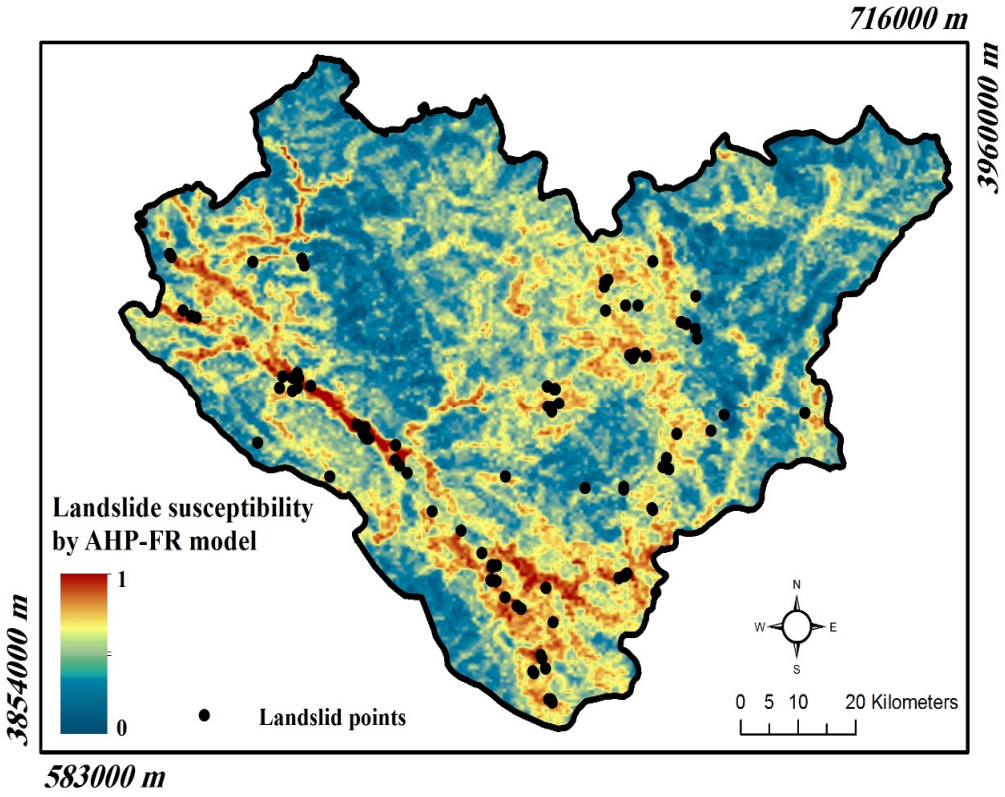

Figure 4. Landslide susceptibility map based on AHP-FR model.

Table 3. Coefficient values for frequency ratio (FR) calculated for relevant classes of 10 criteria.

Factor	Class	Number of landslides	Area of class	Percentage of domain	Percentage of landslide	FR values	Normalised FR values
Geology	Cretaceous	31	14296	55.73	32.98	0.59	**0.23**
	Eocene	26	3754	14.63	27.66	1.89	**0.73**
	Permian	0	48	0.19	0	0	**0**
	Pliocene	0	143	0.56	0	0	**0**
	Quaternary	10	2152	8.39	10.64	1.27	**0.49**
	Triasssic	7	3141	12.24	7.45	0.61	**0.24**
	Oligo-Miocene	20	2120	8.26	21.28	2.57	**1.00**
Land use	Agriculture	50	9589	37.38	53.19	1.42	**1**
	Forest	18	6797	26.50	19.15	0.72	**0.51**
	Iland	0	1	0.00	0	0	**0**
	Rangeland	26	8969	34.96	27.66	0.79	**0.56**
	Urban	0	169	0.66	0	0	**0**
	Waterland	0	127	0.50	0	0	**0**
Climate	Mediterranean	7	6003	23.40	7.45	0.32	**0.17**
	Semi-humid	44	6601	25.73	46.81	1.82	**1**
	Humid	42	10779	42.02	44.68	1.06	**0.58**
	Very humid	1	2271	8.85	1.06	0.12	**0.07**
Erosion	2	0	2770	10.03	0	0	**0**
	3	0	2396	8.68	0	0	**0**
	4	0	327	1.18	0	0	**0**
	5	26	4473	16.20	27.66	1.71	**0.85**
	6	52	11369	41.18	55.32	1.34	**0.67**
	7	15	6127	22.19	15.96	0.72	**0.36**
	9	1	147	0.53	1.06	2.00	**1**
Fault	0-1000	43	9215	35.92	45.74	1.27	**1**
	1000-2000	14	5416	21.11	14.89	0.71	**0.55**
	2000-3000	10	3884	15.14	10.64	0.70	**0.55**
	3000-4000	7	2508	9.78	7.45	0.76	**0.60**
	>4000	20	4631	18.05	21.28	1.18	**0.93**
River	0-500	61	13287	51.79	64.89	1.25	**1**
	500-1000	11	5332	20.78	11.70	0.56	**0.45**
	1000-1500	10	3867	15.07	10.64	0.71	**0.56**
	1500-2000	6	1766	6.88	6.38	0.93	**0.74**
	>2000	6	1402	5.47	6.38	1.17	**0.93**
Aspect	Flat	0	69	0.01	0	0	**0**
	N	12	63244	6.90	12.77	1.85	**1**
	NE	7	126134	13.77	7.45	0.54	**0.29**
	E	7	95634	10.44	7.45	0.71	**0.38**
	SE	8	106908	11.67	8.51	0.73	**0.38**
	S	10	140217	15.30	10.64	0.70	**0.37**
	SW	19	133449	14.56	20.21	1.39	**0.73**
	W	14	98038	10.70	14.89	1.39	**0.73**
	NW	9	98013	10.70	9.57	0.90	**0.47**
Altitude	<1000	1	4526	0.49	1.06	2.15	**0.84**
	1000-1500	40	151378	16.52	42.55	2.58	**1**
	1500-2000	42	507179	55.35	44.68	0.81	**0.31**
	2000-2500	11	234190	25.56	11.70	0.46	**0.18**
	>2500	0	18976	2.07	0	0	**0**
Slope	> 40	24	292334	31.91	25.53	0.80	**0.55**
	40-25	40	325786	35.56	42.55	1.20	**0.82**
	25-10	20	231705	25.29	21.28	0.84	**0.57**
	<10	10	66424	7.25	10.64	1.47	**1**
Road	0-1000	22	3147	12.26	23.40	1.91	**1**
	1000-1500	5	1685	6.57	5.32	0.81	**0.42**
	1500-2000	3	1834	7.15	3.19	0.45	**0.23**
	2000-2500	2	1497	5.83	2.13	0.36	**0.19**
	>2500	62	17501	68.19	65.96	0.97	**0.51**

5.3. Landslide susceptibility mapping using SVM-RBF algorithm

5.3.1. Preparation of training sites

In this work, an RBF-kernel-based SVM (so-called SVM-RBF) data-driven method was used to display regions exhibiting a substantial likelihood of landslide recurrence. The supervised SVM model applied in this part of the study entails two types of training datasets: (1) Landslide locations, which are assigned the value 1 and demonstrate the presence of landslide occurrences and (2) non-landslide locations which are assigned the value 0 and refer to the absence of landslide occurrences. The process of determining and extracting characteristics of landslides is straightforward in areas where there is a large quantity of documented landslide events. The assessment and extraction of non-landslide characteristics pose a significant challenge. For this purpose, there are three crucial factors that necessitate consideration, as follows [24]:

- To improve the classification performance, a balanced dataset with an equal number of landslide and non-landslide instances is crucial.
- It is essential to choose non-landslide locations that are situated at a considerable distance from landslide-prone areas.
- Non-landslide locations have a random or arbitrary nature, as opposed to landslide locations which generally display a grouped or organized character.

This study presents the development of a predictive prospectivity model utilizing the SVM-RBF algorithm. The model incorporates ten key factors, including slope angle, aspect, altitude, geology, land use, climate, erosion, distance to rivers, faults an, and roadways. In order to achieve the intended objective, a dataset consisting of 1200 pixel values was utilized for training purposes. These pixel values were carefully chosen from various locations, encompassing both landslide and non-landslide areas, totaling 94 instances. Therefore, the resulting confusion matrix consists of 11 columns: 10 representing the key factors and one representing the target variable. As previously described, the target variable was assigned a value of 1 for landslide areas and 0 for non-landslide areas. The training dataset consists of 75% of the overall dataset, which amounts to 900 data points. The remaining 25% of the dataset, totaling 300 data points, is designated as Out-Of-Bag (OOB) data. The OOB data is utilized for the purpose of validating the results produced.

5.3.2. Generation of predictive SVM-RBF model

After the preparation of training sites, for optimal selection of the RBF kernel to be used in SVM, two variables, namely C and λ, must be properly tuned. In the present work, various sets of C and λ were tested through a trial-and-error process, and then a trained model was produced for each set. The subsequent phase involved computing the precision of each trained model for every combination of C and λ. Training machine learning algorithms requires a specific subset of the given dataset, known as training data. In this particular instance, training data consisted of established landslide and non-landslide databases. The balance in the number of datasets is a crucial factor in determining the performance of Support Vector Machines (SVM) [130]. Out-of-bag (OOB) data is applied to evaluate the ability of the algorithm after the learning process has been completed. At this stage, it is possible to determine whether the proposed approach has an acceptable performance or not. For validating the SVM methodology, a confusion matrix analysis was performed. This technique is a highly successful strategy for solving binary classification issues [48]. This method can also demonstrate the correlation between the research outcomes and real values. The quantity of correctly and incorrectly categorized data is summed, and the confusion matrix depicts how the susceptibility classification algorithm becomes confused, thereby affecting the correct classification. The 2-class confusion matrix provides a concise summary of four potential outcomes: (a) True Positive (TP), demonstrating the accuracy of the model in defining prospective locations; (b) True Negative (TN), exhibiting the validity of recognizing non- prospective sites; (c) False Positive (FP), where the model mistakenly predicts prospective spots; and (d) False Negative (FN), where the model wrongly anticipates non-prospective areas [50]. A trained model's classification performance can be characterized and formulated as follows [50]:

$$Sensitivity = \frac{TP}{TP + FN} \quad (8)$$

$$Specificity = \frac{TN}{TN + FP} \quad (9)$$

$$\Pr ecision = \frac{TP}{TP + FP} \quad (10)$$

$$Accuracy = \frac{TP + TN}{TP + TN + FP + FN} \quad (11)$$

$$F - measure = \frac{2 \times Sensitivity \times \Pr ecision}{Sensitivity + \Pr ecision} \quad (12)$$

This work employed a total of 1200 pixel values for both training and OOB testing purposes. 75% of the dataset, including a total of 900 instances, was allocated for training purposes, while the remaining 25%, consisting of 300 instances, was reserved for OOB analysis. As shown in Table 4, the trained SVM model exhibits a precision rate of 91.44%, resulting in an 8.56% error, which clearly indicates that the SVM-RBF algorithm exhibits substantial predictive capacity and dependability when employed for the modeling of landslide susceptibility within the designated studied area. Table 4 also provides estimated values for the parameters of the confusion matrix used in the evaluation of SVM techniques. It was found that optimal variable values for the RBF kernel yielding an accuracy of 87.66% (error of 12.34%) (Table 4) are C = 0.1 and λ = 0.25. In the concluding phase, the pixel values of ten key criteria have been collected and employed as test data for the development of a data-driven approach using the developed SVM-RBF approach (Figure 5).

Table 4. Confusion matrix of SVM model for training and OBB dataset.

	TP	TN	FP	FN	Accuracy	Error
Training dataset	407	416	34	43	91.44%	8.56%
OOB dataset	123	140	10	27	87.66%	12.34%

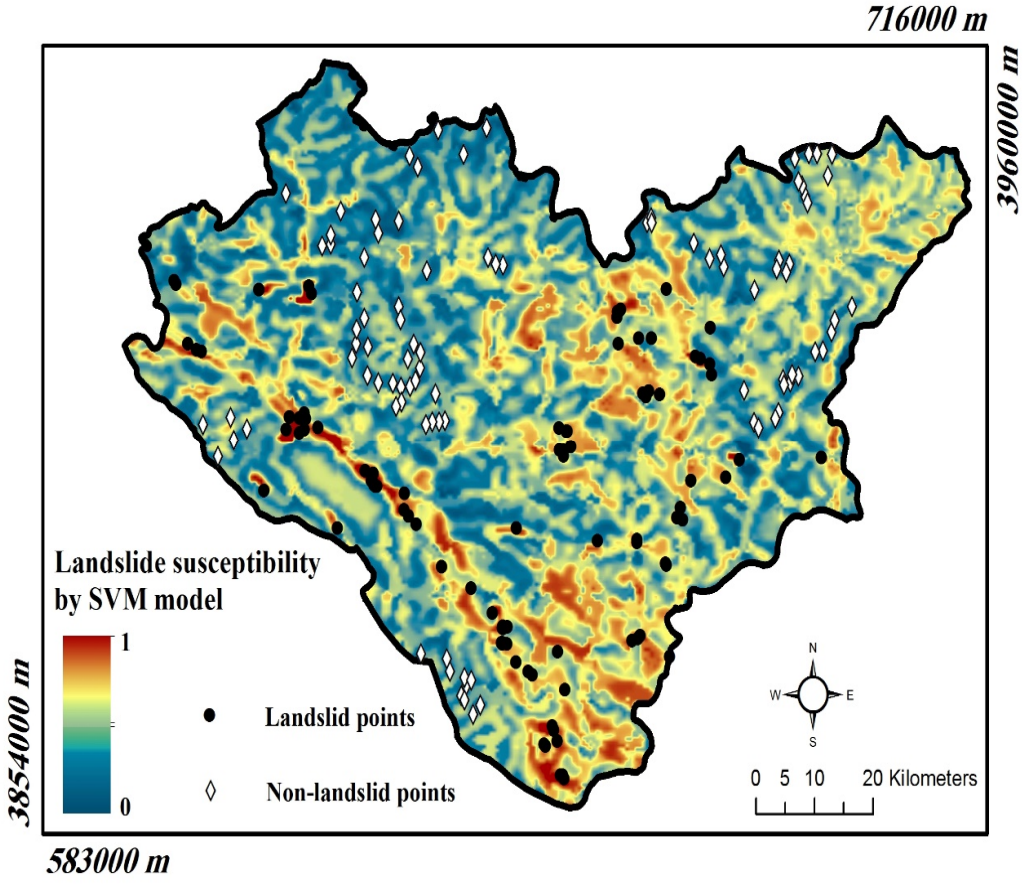

Figure 5. Landslide susceptibility map based on SVM-RBF model.

5.3.3. Validation and evaluation of landslide susceptibility models

To assess the relative efficacy of the FR, AHP-FR, and SVM-RBF algorithms for determining landslide vulnerability, prediction-rate curves were produced (Figure 6). If the derived landslide susceptibility zones maintain a favorable spatial correlation with the spatial positions of

documented landslides, the relevant prediction-rate curve will be placed higher and, thus, the model can be considered efficient. In this regard, the evaluation of FR, AHP-FR, and SVM-RBF methods was performed using prediction-rate curves (Figure 6). It is evident that all three models have demonstrated satisfactory performance in detecting areas prone to landslides, as illustrated in Figures 3, 4, and 5. All the prediction-rate curves of the algorithms lie above the reference line, indicating this. Therefore, it can be concluded that all created models exhibit a high level of reliability in identifying potential areas prone to landslides, thus making them suitable for further investigation and analysis. However, according to Table 5, the prediction-rate curve of the SVM-RBF algorithm, with an AUC value of 84.54%, is significantly higher than those of AHP-FR and FR models, with AUC values of 77.84% and 73.5%, respectively.

Table 5. Results of prediction-rate curves for SVM, AHP-FR and FR models

Model	AUC %
SVM	84.54
AHP-FR	77.84
FR	73.50

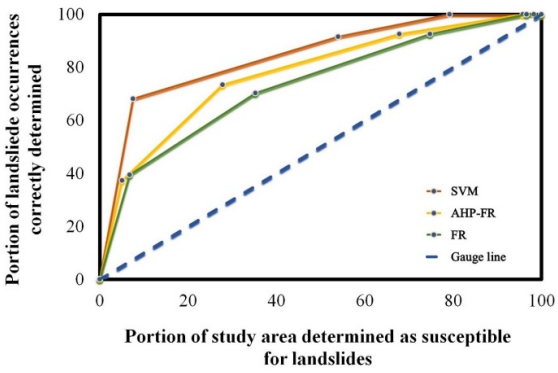

Figure 6. Prediction-rate curves of FR, AHP-FR and SVM-RBF models.

6. Conclusions

The current investigation identified several factors potentially associated with landslide occurrences. The results were used to develop a landslide risk model, applying three methods: AHP, AHP-FR, and SVM-RBF, within the Zarab-Sanandaj sub-basins in Kurdistan province. The assignment of proper weights to each landslide-related factor based on expert opinions using the AHP method, and the calculation of weights for each sub-criterion using the FR procedure, indicated that distance from rivers and the climate factor had the greatest and least impact, respectively, on landslide occurrence within the studied area.

Furthermore, the FR results revealed that the probability of landslides is higher in the Oligo-Miocene geological units and at altitudes between 1000 and 1500 meters. This is likely due to increased precipitation and snow accumulation at higher altitudes, along with the repetitive cycles of glaciation and melting, which increase instability in the region. Conversely, landslide occurrences are less frequent at altitudes between 1500 and 2000 meters, likely due to the presence of more resistant lithological units in those areas.

Additionally, the findings highlight a significant likelihood of landslides in areas that have experienced severe erosion or are located near roads. This is attributed to slope instability caused by excessive erosion, along with unregulated road construction, which results in slope cuts in the region. The models generated to predict landslide susceptibility, using different methods, indicated that landslides are more common in the southern, southwestern, and central regions of the studied area.

In conclusion, the key findings of this study underscore the effectiveness of using weighting methods to identify the most significant factors and even sub-factors that influence landslide occurrences. Both knowledge-driven methods, such as AHP, and data-driven methods, such as the Frequency Ratio (FR), demonstrated their ability to predict landslide-prone areas accurately. However, the use of artificial intelligence-based methods, particularly the Support Vector Machine (SVM) with the Radial Basis Function (RBF) kernel, proved to be far more successful and accurate than the other data-driven and knowledge-based methods. This success is reflected in the success rate curve, a quantitative evaluation tool employed in this study, which confirmed the superior performance of the SVM model in landslide susceptibility mapping. The findings highlight the potential of SVM for providing more reliable predictions, making it a valuable tool for future research in landslide risk assessment and spatial planning in landslide-prone regions.

Building upon these findings, future research in the studied area could focus on the integration of more advanced machine learning techniques, such as deep learning or ensemble models, which could further enhance the predictive accuracy of landslide susceptibility models in this specific region. Additionally, the incorporation of real-time monitoring data, such as precipitation and seismic activity, would likely improve the responsiveness

and dynamism of these models, making them more adaptable to the changing environmental conditions. Furthermore, future studies could explore the development of more localized models tailored to smaller sub-basins or urban areas within the Zarab-Sanandaj sub-basins, where managing landslide risks is crucial for protecting infrastructure. Lastly, investigating the socio-economic impacts of landslides, including costs related to damage and mitigation strategies in this area, could provide valuable insights for policymakers and urban planners.

Acknowledgments

The authors would like to thank Prof. Ataei, the Editor-in-chief and anonymous reviewers for handling this manuscript.

Author Contributions

All authors contributed to the study conception and design. Data collection and modeling were performed by Sarina Akbari, Reza Ghezelbash Hamidreza Ramazi and, Abbas Maghsoudi. The first draft of the manuscript was written by Sarina Akbari. All authors read and approved the final manuscript.

Data Availability

Not applicable

Funding

The authors did not receive support from any organization for the submitted work.

Conflict of Interest Statement

I, the corresponding author, also certify that I have no commercial associations (e.g., consultancies, stock ownership, equity interests, patent-licensing arrangements, etc.) that might pose a conflict of interest in connection with the submitted article, except as disclosed on a separate attachment. All funding sources supporting the work and all institutional or corporate affiliations of mine are acknowledged in a footnote.

References

[1]. Abdo, H. G. (2022). Assessment of landslide susceptibility zonation using frequency ratio and statistical index: a case study of Al-Fawar basin, Tartous, Syria. International Journal of Environmental Science and Technology, 19(4), 2599-2618.

[2]. Abella, E. A. C., & Van Westen, C. J. (2008). Qualitative landslide susceptibility assessment by multicriteria analysis: A case study from San Antonio del Sur, Guantánamo, Cuba. *Geomorphology*, *94*(3-4), 453-466.

[3]. Achu, A. L., Aju, C. D., Pham, Q. B., Reghunath, R., & Anh, D. T. (2022). Landslide susceptibility modelling using hybrid bivariate statistical-based machine-learning method in a highland segment of Southern Western Ghats, India. *Environmental Earth Sciences*, *81*(13), 360.

[4]. Ahmed, B. (2015). Landslide susceptibility mapping using multi-criteria evaluation techniques in Chittagong Metropolitan Area, Bangladesh. *Landslides*, *12*(6), 1077-1095.

[5]. Akbari, S., & Ramazi, H. (2023). Application of AHP-SWOT and geophysical methods to develop a reasonable planning for Zagheh tourist destination considering environmental criteria. *International Journal of Environmental Science*, *8*.

[6]. Akbari, S., Ramazi, H., & Ghezelbash, R. (2023). Using fractal and multifractal methods to reveal geophysical anomalies in Sardouyeh District, Kerman, Iran. *Earth Science Informatics*, *16*(3), 2125-2142.

[7]. Akbari, S., Ramazi, H., & Ghezelbash, R. (2024). A data-driven VIKOR procedure for predictive modeling of porphyry copper prospectivity in SE Iran. *Journal of Geochemical Exploration*, *259*, 107414.

[8]. Akbari, S., Ramazi, H., & Ghezelbash, R. (2025). A novel framework for optimizing the prediction of areas favorable to porphyry-cu mineralization: combination of ant colony and grid search optimization algorithms with support vector machines. *Natural Resources Research*, 1-27.

[9]. Akbari, S., Ramazi, H., Ghezelbash, R., & Maghsoudi, A. (2020). Geoelectrical integrated models for determining the geometry of karstic cavities in the Zarrinabad area, west of Iran: combination of fuzzy logic, CA fractal model and hybrid AHP-TOPSIS procedure. Carbonates and Evaporites, 35, 1-16.

[10]. Aleotti, P. (2004). A warning system for rainfall-induced shallow failures. *Engineering geology*, *73*(3-4), 247-265.

[11]. Aleotti, P., & Chowdhury, R. (1999). Landslide hazard assessment: summary review and new perspectives. *Bulletin of Engineering Geology and the environment*, *58*(1), 21-44.

[12]. Alimoradi, A., Angorani, S., Ebrahimzadeh, M., Shariat Panahi, M., (2011). Magnetic Inverse Modeling of a Dike Using the Artificial Neural Network Approach, The Journal of Near Surface Geophysics (EAGE), 9, 339-347.

[13]. Alimoradi, A., Moradzadeh, A., Bakhtiari, M. R., (2013). Application of Artificial Neural Networks and Support Vector Machines for Carbonate Pores Size Estimation from 3D Seismic Data, Journal of Mining and Environment, 4 (1), 1-14.

[14]. Alimoradi, A., Shahsavani, H., Kamkar Rohani, A., (2011). Prediction of Shear Wave Velocity in Underground Layers Using SASW and Artificial Neural

Networks, The Journal of Engineering (Scientific Research Publishing), 3, 266-275.

[15]. Ayalew, L., & Yamagishi, H. (2005). The application of GIS-based logistic regression for landslide susceptibility mapping in the Kakuda-Yahiko Mountains, Central Japan. *Geomorphology*, *65*(1-2), 15-31.

[16]. Azarafza, M., Azarafza, M., Akgün, H., Atkinson, P. M., & Derakhshani, R. (2021). Deep learning-based landslide susceptibility mapping. *Scientific reports*, *11*(1), 24112.

[17]. Bai, S. B., Wang, J., Lü, G. N., Zhou, P. G., Hou, S. S., & Xu, S. N. (2010). GIS-based logistic regression for landslide susceptibility mapping of the Zhongxian segment in the Three Gorges area, China. *Geomorphology*, *115*(1-2), 23-31.

[18]. Bednarik, M., Magulová, B., Matys, M., & Marschalko, M. (2010). Landslide susceptibility assessment of the Kraľovany–Liptovský Mikuláš railway case study. *Physics and Chemistry of the Earth, Parts A/B/C*, *35*(3-5), 162-171.

[19]. Bednarik, M., Yilmaz, I., & Marschalko, M. (2012). Landslide hazard and risk assessment: a case study from the Hlohovec–Sered'landslide area in south-west Slovakia. *Natural hazards*, *64*(1), 547-575.

[20]. Bhardwaj, V., & Singh, K. (2023). Landslide Susceptibility Assessment using Remote Sensing and GIS-a Review. Journal of Mining and Environment, 14(1), 133-154.

[21]. Broeckx, J., Vanmaercke, M., Duchateau, R., & Poesen, J. (2018). A data-based landslide susceptibility map of Africa. *Earth-Science Reviews*, *185*, 102-121.

[22]. Burges, C. J. (1998). A tutorial on support vector machines for pattern recognition. *Data mining and knowledge discovery*, *2*(2), 121-167.

[23]. Cao, Y., Wei, X., Fan, W., Nan, Y., Xiong, W., & Zhang, S. (2021). Landslide susceptibility assessment using the Weight of Evidence method: A case study in Xunyang area, China. *PLoS one*, *16*(1), e0245668.

[24]. Carranza, E. J. M., Van Ruitenbeek, F. J. A., Hecker, C., van der Meijde, M., & van der Meer, F. D. (2008). Knowledge-guided data-driven evidential belief modeling of mineral prospectivity in Cabo de Gata, SE Spain. *International Journal of Applied Earth Observation and Geoinformation*, *10*(3), 374-387.

[25]. Castro-Miguel, R., Legorreta-Paulín, G., Bonifaz-Alfonzo, R., Aceves-Quesada, J. F., & Castillo-Santiago, M. Á. (2022). Modeling spatial landslide susceptibility in volcanic terrains through continuous neighborhood spatial analysis and multiple logistic regression in La Ciénega watershed, Nevado de Toluca, Mexico. *Natural Hazards*, *113*(1), 767-788.

[26]. Chauhan, S., Sharma, M., Arora, M. K., & Gupta, N. K. (2010). Landslide susceptibility zonation through ratings derived from artificial neural network. *International Journal of Applied Earth Observation and Geoinformation*, *12*(5), 340-350.

[27]. Chen, Wei, et al. "Landslide susceptibility modelling using GIS-based machine learning techniques for Chongren County, Jiangxi Province, China." *Science of the total environment* 626 (2018): 1121-1135.

[28]. Ciabatta, L., Camici, S., Brocca, L., Ponziani, F., Stelluti, M., Berni, N., & Moramarco, T. J. J. O. H. (2016). Assessing the impact of climate-change scenarios on landslide occurrence in Umbria Region, Italy. *Journal of Hydrology*, *541*, 285-295.

[29]. Clerici, A., Perego, S., Tellini, C., & Vescovi, P. (2002). A procedure for landslide susceptibility zonation by the conditional analysis method. *Geomorphology*, *48*(4), 349-364.

[30]. Conoscenti, C., Ciaccio, M., Caraballo-Arias, N. A., Gómez-Gutiérrez, Á., Rotigliano, E., & Agnesi, V. (2015). Assessment of susceptibility to earth-flow landslide using logistic regression and multivariate adaptive regression splines: a case of the Belice River basin (western Sicily, Italy). *Geomorphology*, *242*, 49-64.

[31]. Cristianini, N., & Shawe-Taylor, J. (2000). An introduction to support vector machines and other kernel-based learning methods. Cambridge university press.

[32]. Dai, F. C., Lee, C. F., & Ngai, Y. Y. (2002). Landslide risk assessment and management: an overview. *Engineering geology*, *64*(1), 65-87.

[33]. Dai, F. C., Lee, C. F., Li, J. X. Z. W., & Xu, Z. W. (2001). Assessment of landslide susceptibility on the natural terrain of Lantau Island, Hong Kong. *Environmental Geology*, *40*(3), 381-391.

[34]. Das, S., Sarkar, S., & Kanungo, D. P. (2022). GIS-based landslide susceptibility zonation mapping using the analytic hierarchy process (AHP) method in parts of Kalimpong Region of Darjeeling Himalaya. Environmental Monitoring and Assessment, 194(4), 234.

[35]. Daviran, M., Shamekhi, M., Ghezelbash, R., & Maghsoudi, A. (2023). Landslide susceptibility prediction using artificial neural networks, SVMs and random forest: hyperparameters tuning by genetic optimization algorithm. International Journal of Environmental Science and Technology, 20(1), 259-276.

[36]. Demir, G., Aytekin, M., Akgün, A., Ikizler, S. B., & Tatar, O. (2013). A comparison of landslide susceptibility mapping of the eastern part of the North Anatolian Fault Zone (Turkey) by likelihood-frequency ratio and analytic hierarchy process methods. *Natural hazards*, *65*(3), 1481-1506.

[37]. Dhakal, D., & Singh, K. (2025). A Geospatial Approach to Landslide Susceptibility Mapping of Spiti, India. Journal of Mining and Environment, Vol. 16, No. 1, 2025.

[38]. Dong, J. J., Lee, W. R., Lin, M. L., Huang, A. B., & Lee, Y. L. (2009). Effects of seismic anisotropy and geological characteristics on the kinematics of the neighboring Jiufengershan and Hungtsaiping landslides during Chi-Chi earthquake. *Tectonophysics*, *466*(3-4), 438-457.

[39]. Dou, J., Tien Bui, D., P. Yunus, A., Jia, K., Song, X., Revhaug, I., ... & Zhu, Z. (2015). Optimization of causative factors for landslide susceptibility evaluation using remote sensing and GIS data in parts of Niigata, Japan. PloS one, 10(7), e0133262.

[40]. Duman, T. Y., Can, T., Gokceoglu, C., Nefeslioglu, H. A., & Sonmez, H. (2006). Application of logistic regression for landslide susceptibility zoning of Cekmece Area, Istanbul, Turkey. *Environmental Geology*, *51*(2), 241-256.

[41]. Ercanoglu, M. U. R. A. T., Gokceoglu, C. A. N. D. A. N., & Van Asch, T. W. (2004). Landslide susceptibility zoning north of Yenice (NW Turkey) by multivariate statistical techniques. *Natural Hazards*, *32*(1), 1-23.

[42]. Ercanoglu, M., & Gokceoglu, C. (2004). Use of fuzzy relations to produce landslide susceptibility map of a landslide prone area (West Black Sea Region, Turkey). *Engineering Geology*, *75*(3-4), 229-250.

[43]. Felicísimo, Á. M., Cuartero, A., Remondo, J., & Quirós, E. (2013). Mapping landslide susceptibility with logistic regression, multiple adaptive regression splines, classification and regression trees, and maximum entropy methods: a comparative study. *Landslides*, *10*(2), 175-189.

[44]. Fernández, C. I., Del Castillo, T. F., Hamdouni, R. E., & Montero, J. C. (1999). Verification of landslide susceptibility mapping: a case study. *Earth Surface Processes and Landforms: The Journal of the British Geomorphological Research Group*, *24*(6), 537-544.

[45]. Fressard, M., Thiery, Y., & Maquaire, O. (2014). Which data for quantitative landslide susceptibility mapping at operational scale? Case study of the Pays d'Auge plateau hillslopes (Normandy, France). *Natural Hazards and Earth System Sciences*, *14*(3), 569-588.

[46]. Ghasemi Tabar, H. R., Alimoradi, A., Hemmati Ahooi, H. R., Fathi, M. (2023). Intelligent borehole simulation with python programming, Journal of Mining and Environment, doi: 10.22044/jme.2023.13610.2527.

[47]. Ghezelbash, R., & Maghsoudi, A. (2018). A hybrid AHP-VIKOR approach for prospectivity modeling of porphyry Cu deposits in the Varzaghan District, NW Iran. Arabian Journal of Geosciences, 11, 1-15.

[48]. Ghezelbash, R., Daviran, M., Maghsoudi, A., Ghaeminejad, H., & Niknezhad, M. (2023). Incorporating the genetic and firefly optimization algorithms into K-means clustering method for detection of porphyry and skarn Cu-related geochemical footprints in Baft district, Kerman, Iran. *Applied Geochemistry*, *148*, 105538.

[49]. Ghezelbash, R., Maghsoudi, A., & Daviran, M. (2019). Implementation of Fuzzy-AHP and Fuzzy-GAMMA approaches for discovering the prospectivity areas of Au mineralization in Takhte-Soleyman district. Researches in Earth Sciences, 10(1), 143-162.

[50]. Ghezelbash, R., Maghsoudi, A., Shamekhi, M., Pradhan, B., & Daviran, M. (2023). Genetic algorithm to optimize the SVM and K-means algorithms for mapping of mineral prospectivity. Neural Computing and Applications, 35(1), 719-733.

[51]. Gökceoglu, C., & Aksoy, H. Ü. S. E. Y. İ. N. (1996). Landslide susceptibility mapping of the slopes in the residual soils of the Mengen region (Turkey) by deterministic stability analyses and image processing techniques. *Engineering Geology*, *44*(1-4), 147-161.

[52]. Gupta, R. P., Saha, A. K., Arora, M. K., & Kumar, A. (1999). Landslide Hazard Zonation in a part of the Bhagirathi Valley. *Garhwal Mimalyas, using integrated remote sensing–GIS, Himalayan Geology*, *20*, 71-85.

[53]. Hemasinghe, H., Rangali, R. S. S., Deshapriya, N. L., & Samarakoon, L. (2018). Landslide susceptibility mapping using logistic regression model (a case study in Badulla District, Sri Lanka). Procedia engineering, 212, 1046-1053.

[54]. Hillman, A. L., Yu, J., Abbott, M. B., Cooke, C. A., Bain, D. J., & Steinman, B. A. (2014). Rapid environmental change during dynastic transitions in Yunnan Province, China. *Quaternary Science Reviews*, *98*, 24-32.

[55]. Hong, H., Chen, W., Xu, C., Youssef, A. M., Pradhan, B., & Tien Bui, D. (2017). Rainfall-induced landslide susceptibility assessment at the Chongren area (China) using frequency ratio, certainty factor, and index of entropy. *Geocarto international*, *32*(2), 139-154.

[56]. Hong, H., Pradhan, B., Xu, C., & Bui, D. T. (2015). Spatial prediction of landslide hazard at the Yihuang area (China) using two-class kernel logistic regression, alternating decision tree and support vector machines. *Catena*, *133*, 266-281.

[57]. Huang, F., Chen, J., Liu, W., Huang, J., Hong, H., & Chen, W. (2022). Regional rainfall-induced landslide hazard warning based on landslide susceptibility mapping and a critical rainfall threshold. *Geomorphology*, *408*, 108236.

[58]. Jaafari, A., Najafi, A., Pourghasemi, H. R., Rezaeian, J., & Sattarian, A. (2014). GIS-based frequency ratio and index of entropy models for landslide susceptibility assessment in the Caspian forest, northern Iran. *International Journal of Environmental Science and Technology*, *11*(4), 909-926.

[59]. Jebur, M. N., Pradhan, B., & Tehrany, M. S. (2015). Using ALOS PALSAR derived high-resolution DInSAR to detect slow-moving landslides in tropical forest: Cameron Highlands, Malaysia. *Geomatics, Natural Hazards and Risk*, *6*(8), 741-759.

[60]. Kanwal, S., Atif, S., & Shafiq, M. (2017). GIS based landslide susceptibility mapping of northern areas of Pakistan, a case study of Shigar and Shyok Basins. *Geomatics, Natural Hazards and Risk*, *8*(2), 348-366.

[61]. Kavzoglu, T., & Colkesen, I. (2014). A comparison of SVM and other classifiers for landslide susceptibility mapping. Environmental Earth Sciences, 72(6), 2011-2024. https://doi.org/10.1007/s12665-014-3636-0

[62]. Kavzoglu, T., Sahin, E. K., & Colkesen, I. (2014). Landslide susceptibility mapping using GIS-based multi-

criteria decision analysis, support vector machines, and logistic regression. Landslides, 11, 425-439.

[63]. Kavzoglu, T., Sahin, E. K., & Colkesen, I. (2015). Selecting optimal conditioning factors in shallow translational landslide susceptibility mapping using genetic algorithm. *Engineering Geology*, *192*, 101-112.

[64]. Kayastha, P., Dhital, M. R., & De Smedt, F. (2013). Application of the analytical hierarchy process (AHP) for landslide susceptibility mapping: A case study from the Tinau watershed, west Nepal. Computers & Geosciences, 52, 398-408.

[65]. Kecman, V. (2005). Support vector machines–an introduction. In *Support vector machines: theory and applications* (pp. 1-47). Springer, Berlin, Heidelberg.

[66]. Keefer, D. K., Wilson, R. C., Mark, R. K., Brabb, E. E., Brown, W. M., Ellen, S. D., ... & Zatkin, R. S. (1987). Real-time landslide warning during heavy rainfall. *Science*, *238*(4829), 921-925.

[67]. Khan, H., Shafique, M., Khan, M. A., Bacha, M. A., Shah, S. U., & Calligaris, C. (2019). Landslide susceptibility assessment using Frequency Ratio, a case study of northern Pakistan. *The Egyptian Journal of Remote Sensing and Space Science*, *22*(1), 11-24.

[68]. Kornejady, A., Heidari, K., & Nakhavali, M. (2015). Assessment of landslide susceptibility, semi-quantitative risk and management in the Ilam dam basin, Ilam, Iran. Environmental Resources Research, 3(1), 85-109.

[69]. Kornejady, A., Ownegh, M., & Bahremand, A. (2017). Landslide susceptibility assessment using maximum entropy model with two different data sampling methods. *Catena*, *152*, 144-162.

[70]. Lee S (2005) Application of logistic regression model and its validation for landslide susceptibility mapping using GIS and remote sensing data. Int J Remote Sens 26:1477–1491.

[71]. Lee S, Choi J, Min K (2004a) Probabilistic landslide hazard mapping using GIS and remote sensing data at Boun, Korea. Int J Remote Sens 25:2037–2052.

[72]. Lee, C. H., & Hsu, S. H. (2017). Landslide susceptibility mapping using support vector machine: A case study in the Lushan, Taiwan area. Geomatics, Natural Hazards and Risk, 8(4), 346-361. https://doi.org/10.1080/19475705.2016.1217227

[73]. Lee, S., & Sambath, T. (2006). Landslide susceptibility mapping in the Damrei Romel area, Cambodia using frequency ratio and logistic regression models. Environmental Geology, 50, 847-855.

[74]. Lee, S., Hong, S. M., & Jung, H. S. (2017). A support vector machine for landslide susceptibility mapping in Gangwon Province, Korea. Sustainability, 9(1), 48.

[75]. Leonardi, G., Palamara, R., & Cirianni, F. (2016). Landslide susceptibility mapping using a fuzzy approach. *Procedia engineering*, *161*, 380-387.

[76]. Li, L., Lan, H., Guo, C., Zhang, Y., Li, Q., & Wu, Y. (2017). A modified frequency ratio method for landslide susceptibility assessment. Landslides, 14, 727-741.

[77]. Li, Z., Nadim, F., Huang, H., Uzielli, M., & Lacasse, S. (2010). Quantitative vulnerability estimation for scenario-based landslide hazards. *Landslides*, *7*(2), 125-134.

[78]. Liu, Q., & Tang, A. (2022). Exploring aspects affecting the predicted capacity of landslide susceptibility based on machine learning technology. *Geocarto International*, *37*(26), 14547-14569.

[79]. Mahvash Mohammadi, N., & Hezarkhani, A. (2020). A comparative study of SVM and RF methods for classification of alteration zones using remotely sensed data. Journal of Mining and Environment, 11(1), 49-61.

[80]. Mandal, B., & Mandal, S. (2018). Analytical hierarchy process (AHP) based landslide susceptibility mapping of Lish river basin of eastern Darjeeling Himalaya, India. *Advances in Space Research*, *62*(11), 3114-3132.

[81]. Marjanović, M., Kovačević, M., Bajat, B., & Voženílek, V. (2011). Landslide susceptibility assessment using SVM machine learning algorithm. Engineering Geology, 123(3), 225-234.

[82]. Moosavi, M., & Pakdaman, A. M. (2024). New 2D joint roughness profiles based on pattern recognition technique. *Bulletin of Engineering Geology and the Environment*, *83*(1), 4.

[83]. Ocakoglu F, Gokceoglu C, Ercanoglu M (2002) Dynamics of a complex mass movement triggered by heavy rainfall: a case study from NW Turkey. Geomorphology 42(3):329–341.

[84]. Oliveira, S. C., Zêzere, J. L., Catalão, J., & Nico, G. (2015). The contribution of PSInSAR interferometry to landslide hazard in weak rock-dominated areas. *Landslides*, *12*(4), 703-719.

[85]. Pachauri, A. K., Gupta, P. V., & Chander, R. (1998). Landslide zoning in a part of the Garhwal Himalayas. *Environmental Geology*, *36*(3), 325-334.

[86]. Pakdaman, A. M., & Moosavi, M. (2023). Surface roughness assessment of natural rock joints based on an unsupervised pattern recognition technique using 2D profiles. *Rudarsko-geološko-naftni zbornik*, *38*(2), 185-198.

[87]. Pakdaman, A. M., & Moosavi, M. (2024). Determination of surface roughness of rocks based on 2D profiles using machine learning methods. *Archive of Applied Mechanics*, *94*(1), 157-185.

[88]. Park, S., Choi, C., Kim, B., & Kim, J. (2013). Landslide susceptibility mapping using frequency ratio, analytic hierarchy process, logistic regression, and artificial neural network methods at the Inje area, Korea. Environmental earth sciences, 68, 1443-1464.

[89]. Pourghasemi, H. R., & Kerle, N. (2016). Random forests and evidential belief function-based landslide

susceptibility assessment in Western Mazandaran Province, Iran. *Environmental earth sciences*, *75*(3), 185.

[90]. Pourghasemi, H. R., & Rossi, M. (2017). Landslide susceptibility modeling in a landslide prone area in Mazandarn Province, north of Iran: a comparison between GLM, GAM, MARS, and M-AHP methods. *Theoretical and Applied Climatology*, *130*(1), 609-633.

[91]. Pourghasemi, H. R., Gayen, A., Park, S., Lee, C. W., & Lee, S. (2018). Assessment of landslide-prone areas and their zonation using logistic regression, logitboost, and naïvebayes machine-learning algorithms. *Sustainability*, *10*(10), 3697.

[92]. Pourghasemi, H. R., Pradhan, B., & Gokceoglu, C. (2012). Application of fuzzy logic and analytical hierarchy process (AHP) to landslide susceptibility mapping at Haraz watershed, Iran. *Natural hazards*, *63*(2), 965-996.

[93]. Pradhan B (2010a) Remote sensing and GIS-based landslide hazard analysis and cross-validation using multivariate logistic regression model on three test areas in Malaysia. Adv Space Res 45:1244–1256.

[94]. Pradhan B (2010b) Use of GIS-based fuzzy logic relations and its cross application to produce landslide susceptibility maps in three test areas in Malaysia. Environ Earth Sci. doi:10.1007/s12665-010-0705-1.

[95]. Pradhan, B. (2010). Landslide susceptibility mapping of a catchment area using frequency ratio, fuzzy logic and multivariate logistic regression approaches. *Journal of the Indian Society of Remote Sensing*, *38*(2), 301-320.

[96]. Pradhan, B. (2013). A comparative study on the predictive ability of the decision tree, support vector machine and neuro-fuzzy models in landslide susceptibility mapping using GIS. *Computers & Geosciences*, *51*, 350-365.

[97]. Pradhan, B., & Lee, S. (2010). Landslide susceptibility assessment and factor effect analysis: backpropagation artificial neural networks and their comparison with frequency ratio and bivariate logistic regression modelling. *Environmental Modelling & Software*, *25*(6), 747-759.

[98]. Rai, D. K., Xiong, D., Zhao, W., Zhao, D., Zhang, B., Dahal, N. M., ... & Baig, M. A. (2022). An investigation of landslide susceptibility using logistic regression and statistical index methods in Dailekh District, Nepal. *Chinese Geographical Science*, *32*(5), 834-851.

[99]. Reichenbach, P., Rossi, M., Malamud, B. D., Mihir, M., & Guzzetti, F. (2018). A review of statistically-based landslide susceptibility models. *Earth-science reviews*, *180*, 60-91.

[100]. Reichenbach, P., Busca, C., Mondini, A. C., & Rossi, M. (2014). The influence of land use change on landslide susceptibility zonation: the Briga catchment test site (Messina, Italy). *Environmental management*, *54*, 1372-1384.

[101]. Remondo, J., Bonachea, J., & Cendrero, A. (2005). A statistical approach to landslide risk modelling at basin scale: from landslide susceptibility to quantitative risk assessment. *Landslides*, *2*, 321-328.

[102]. Ruff, M., & Czurda, K. (2008). Landslide susceptibility analysis with a heuristic approach in the Eastern Alps (Vorarlberg, Austria). *Geomorphology*, *94*(3-4), 314-324.

[103]. Saaty, T. L. (1994). How to make a decision: the analytic hierarchy process. *Interfaces*, *24*(6), 19-43.

[104]. Saha, A. K., Gupta, R. P., & Arora, M. K. (2002). GIS-based landslide hazard zonation in the Bhagirathi (Ganga) valley, Himalayas. *International journal of remote sensing*, *23*(2), 357-369.

[105]. Saha, A. K., Gupta, R. P., Sarkar, I., Arora, M. K., & Csaplovics, E. (2005). An approach for GIS-based statistical landslide susceptibility zonation—with a case study in the Himalayas. *Landslides*, *2*(1), 61-69.

[106]. Sarina Akbari, Hamidreza Ramazi. (2023) Application of AHP -SWOT and Geophysical Methods to Develop a Reasonable Planning for Zagheh Tourist Destination Considering Environmental Criteria. International Journal of Environmental Science, 8, 11-56.

[107]. Shahabi, H., & Hashim, M. (2015). Landslide susceptibility mapping using GIS-based statistical models and Remote sensing data in tropical environment. *Scientific reports*, *5*(1), 1-15.

[108]. Shahabi, H., Hashim, M., & Ahmad, B. B. (2015). Remote sensing and GIS-based landslide susceptibility mapping using frequency ratio, logistic regression, and fuzzy logic methods at the central Zab basin, Iran. *Environmental Earth Sciences*, *73*(12), 8647-8668.

[109]. Shahri, A. A., Spross, J., Johansson, F., & Larsson, S. (2019). Landslide susceptibility hazard map in southwest Sweden using artificial neural network. *Catena*, *183*, 104225.

[110]. Singh, A., Pal, S., & Kanungo, D. P. (2021). An integrated approach for landslide susceptibility–vulnerability–risk assessment of building infrastructures in hilly regions of India. *Environment, Development and Sustainability*, *23*(4), 5058-5095.

[111]. Taner San, B. (2014). An evaluation of SVM using polygon-based random sampling in landslide susceptibility mapping: The Candir catchment area (western Antalya, Turkey). International journal of applied earth observation and geoinformation, 26, 399-412.

[112]. Tsangaratos, P., & Ilia, I. (2016). Comparison of a logistic regression and Naïve Bayes classifier in landslide susceptibility assessments: The influence of models complexity and training dataset size. *Catena*, *145*, 164-179.

[113]. Tsangaratos, P., Ilia, I., Hong, H., Chen, W., & Xu, C. (2017). Applying Information Theory and GIS-based quantitative methods to produce landslide susceptibility maps in Nancheng County, China. *Landslides*, *14*(3), 1091-1111.

[114]. Van Den Eeckhaut, M., & Hervás, J. (2012). State of the art of national landslide databases in Europe and their potential for assessing landslide susceptibility, hazard and risk. *Geomorphology*, *139*, 545-558.

[115]. Van Westen, C. J., & Alzate Bonilla, J. B. (1990). Mountain hazard analysis using a PC-based GIS. In *International congress international association of engineering geology. 6* (pp. 265-271).

[116]. Van Westen, C. J., Rengers, N., & Soeters, R. (2003). Use of geomorphological information in indirect landslide susceptibility assessment. *Natural hazards*, *30*, 399-419.

[117]. Vapnik V N 1995 *The Nature of Statistical Learning Theory* (New York: Springer Verlag).

[118]. Wang, L. J., Guo, M., Sawada, K., Lin, J., & Zhang, J. (2015). Landslide susceptibility mapping in Mizunami City, Japan: A comparison between logistic regression, bivariate statistical analysis and multivariate adaptive regression spline models. *Catena*, *135*, 271-282.

[119]. Wang, Z., Wang, D., Guo, Q., & Wang, D. (2020). Regional landslide hazard assessment through integrating susceptibility index and rainfall process. *Natural Hazards*, *104*(3), 2153-2173.

[120]. Wind, Y., & Saaty, T. L. (1980). Marketing applications of the analytic hierarchy process. *Management science*, *26*(7), 641-658.

[121]. Xu, C., Dai, F., Xu, X., & Lee, Y. H. (2012). GIS-based support vector machine modeling of earthquake-triggered landslide susceptibility in the Jianjiang River watershed, China. Geomorphology, 145, 70-80.

[122]. Yalcin, A. (2008). GIS-based landslide susceptibility mapping using analytical hierarchy process and bivariate statistics in Ardesen (Turkey): comparisons of results and confirmations. *Catena*, *72*(1), 1-12.

[123]. Yalcin, A., & Bulut, F. (2007). Landslide susceptibility mapping using GIS and digital photogrammetric techniques: a case study from Ardesen (NE-Turkey). *Natural Hazards*, *41*(1), 201-226.

[124]. Yao, X., Tham, L. G., & Dai, F. C. (2008). Landslide susceptibility mapping based on support vector machine: a case study on natural slopes of Hong Kong, China. *Geomorphology*, *101*(4), 572-582.

[125]. Yilmaz, I. (2009). Landslide susceptibility mapping using frequency ratio, logistic regression, artificial neural networks and their comparison: a case study from Kat landslides (Tokat—Turkey). Computers & Geosciences, 35(6), 1125-1138.

[126]. Yilmaz, I. (2010). Comparison of landslide susceptibility mapping methodologies for Koyulhisar, Turkey: conditional probability, logistic regression, artificial neural networks, and support vector machine. *Environmental Earth Sciences*, *61*(4), 821-836.

[127]. Youssef, A. M., Al-Kathery, M., & Pradhan, B. (2015). Landslide susceptibility mapping at Al-Hasher area, Jizan (Saudi Arabia) using GIS-based frequency ratio and index of entropy models. *Geosciences Journal*, *19*(1), 113-134.

[128]. Yu, X., Zhang, K., Song, Y., Jiang, W., & Zhou, J. (2021). Study on landslide susceptibility mapping based on rock–soil characteristic factors. *Scientific reports*, *11*(1), 15476.

[129]. Zhang, C., Li, Z., Yu, C., Chen, B., Ding, M., Zhu, W., ... & Peng, J. (2022). An integrated framework for wide-area active landslide detection with InSAR observations and SAR pixel offsets. *Landslides*, *19*(12), 2905-2923.

[130]. Zuo, R., & Carranza, E. J. M. (2011). Support vector machine: A tool for mapping mineral prospectivity. *Computers & Geosciences*, *37*(12), 1967-1975.

نشریه مهندسی معدن و محیط زیست
نشانی نشریه: www.jme.shahroodut.ac.ir
انجمن مهندسی معدن ایران
دانشگاه صنعتی شاهرود

پهنه‌بندی حساسیت زمین‌لغزش: مقایسه روش‌های دانش‌محور AHP-FR و داده‌محور SVM در زیرحوضه‌های زراب–سنندج، استان کردستان، ایران

سارینا اکبری[1]، رضا قزلباش[2*]، حمیدرضا رمضی[1] و عباس مقصودی[1]

۱ -دانشکده مهندسی معدن، دانشگاه صنعتی امیرکبیر، تهران، ایران
۲- دانشکدگان فنی دانشگاه تهران، تهران، ایران

اطلاعات مقاله

تاریخ ارسال: ۲۰۲۴/۰۹/۲۵
تاریخ داوری: ۲۰۲۵/۰۴/۱۱
تاریخ پذیرش: ۲۰۲۵/۰۵/۰۵

DOI: 10.22044/jme.2025.15122.2890

کلمات کلیدی

زمین‌لغزش
فرایند تحلیل سلسله‌مراتبی
نسبت فراوانی
ماشین بردار پشتیبان
کردستان

چکیده

خطرات طبیعی، به‌ویژه زمین‌لغزش‌ها، همواره به‌عنوان یکی از چالش‌های جدی برای جوامع انسانی، زیرساخت‌ها و محیط‌زیست مطرح بوده‌اند. بر این اساس، برنامه‌ریزی اصولی در حوزه توسعه پایدار شهری و روستایی مستلزم تدوین و به‌کارگیری مدل‌های دقیق پهنه‌بندی خطر زمین‌لغزش است. در سال‌های اخیر، رویکردهای متنوعی به‌منظور تهیه نقشه‌های خطر زمین‌لغزش پیشنهاد شده‌اند که می‌توانند نقش بسزایی در پیش‌بینی نواحی مستعد وقوع این پدیده ایفا نمایند. پژوهش حاضر با بهره‌گیری از رویکردی تلفیقی، به ترکیب روش‌های آماری و تصمیم‌گیری چندمعیاره (MCDM) پرداخته است. در این چارچوب، نسبت فراوانی (FR) و فرایند تحلیل سلسله‌مراتبی (AHP) به‌عنوان روش‌های مبتنی بر دانش کارشناسی، و الگوریتم ماشین بردار پشتیبان (SVM) با تابع کرنل RBF به‌عنوان یک روش داده‌محور در حوزه یادگیری ماشین مورد استفاده قرار گرفتند. ده عامل مؤثر در وقوع زمین‌لغزش شامل شیب، جهت شیب، ارتفاع، زمین‌شناسی، کاربری اراضی، اقلیم، شدت فرسایش، و فاصله از رودخانه، گسل و جاده در فرآیند مدل‌سازی لحاظ گردیدند. نتایج حاصل حاکی از آن است که نواحی جنوبی، جنوب‌غربی و مرکزی منطقه مورد مطالعه بیش‌ترین پتانسیل وقوع زمین‌لغزش را دارا می‌باشند. ارزیابی عملکرد مدل‌ها از طریق تحلیل منحنی نرخ پیش‌بینی (PRC) نشان داد که الگوریتم SVM دقت بالاتری در شناسایی نواحی مستعد نسبت به مدل‌های FR و AHP-FR دارد. یافته‌های این تحقیق می‌تواند به‌عنوان مبنایی علمی در راستای کاهش مخاطرات احتمالی آتی و مدیریت ریسک زمین‌لغزش در برنامه‌ریزی‌های محیطی مورد بهره‌برداری قرار گیرد.

نویسنده مسئول مکاتبات: r.ghezelbash@ut.ac.ir (ر. قزلباش)